available at www.sciencedirect.com

ScienceDirect

journal homepage: www.elsevier.com/locate/chnjc

Article

Photocatalytic degradation of methylene blue by MoO_3 modified TiO_2 under visible light

Huabo Yang [a], Xiang Li [a,b,*], Anjie Wang [a,b], Yao Wang [b], Yongying Chen [b]

[a] *State Key Laboratory of Fine Chemicals, School of Chemical Engineering, Dalian University of Technology, Dalian 116024, Liaoning, China*
[b] *Liaoning Key Laboratory of Petrochemical Technology and Equipments, Dalian 116024, Liaoning, China*

ARTICLE INFO

Article history:
Received 14 July 2013
Accepted 9 October 2013
Published 20 January 2014

Keywords:
Titania
Molybdenum oxide
Incipient impregnation
Methylene blue
Visible light

ABSTRACT

MoO_3/P25 catalysts were prepared by an impregnation method. The catalysts were characterized by X-ray diffraction, ultraviolet-visible spectrophotometry, Fourier transform infrared spectroscopy, and laser Raman spectroscopy, and their photocatalytic activty was evaluated by the degradation of methylene blue dye under visible light. The monolayer dispersion threshold of MoO_3 on P25 was around 0.1 g/g. The strong interaction between the monolayer-dispersed tetrahedral-coordinated molybdenum oxide species and P25 led to a decrease in the band gap of P25, thus increasing the visible light absorption of the catalyst. Crystalline MoO_3 was formed on catalysts with a MoO_3/P25 mass ratio above 0.1. In these cases, the visible light absorption of the catalysts decreased with increasing MoO_3 content. The band gap of the catalyst was not the only factor affecting its photocatalytic activity for the degradation of methylene blue under visible light. MoO_3/P25 with the MoO_3 to P25 mass ratio of 0.25, which possessed not only suitable band gap but also a certain amount of crystalline MoO_3, showed the best catalytic performance.

1. Introduction

TiO_2 is the most frequently used photocatalyst due to its low cost, high stability, and high photocatalytic oxidation activity. In the presence of TiO_2, most organic pollutants can be photocatalytically degraded and mineralized to CO_2, H_2O, and other small inorganic molecules. However, TiO_2 has a relatively large band gap (3.0–3.2 eV), requiring high energy ultraviolet (UV) light for activation, and also suffers from low quantum yield. Hence, most of the efforts towards modifying TiO_2 to enhance its visible light absorption and solar energy conversion efficiency have been devoted to reducing its band gap and improving its quantum efficiency. The reported methods include metal deposition [1,2], ion doping [3], coupling with other semiconductors [4], and organic photosensitization [5]. The band gap of MoO_3 is 2.9 eV, which is close to that of TiO_2, and strong interactions occur between MoO_3 and TiO_2 [6]. Many studies have indicated that the photocatalytic activity of TiO_2 in the UV region or the visible light region can be improved by MoO_3 doping. For example, Kubacka et al. [7] studied mixed Ti-M (M = V, Mo, Nb, and W) oxides and reported that only structurally highly homogeneous anatase-type oxides with electronic properties exclusively producing a decrease in band gap may lead to efficient visible light-driven photocatalysts.

* Corresponding author. Tel: +86-411-84986124; Fax: +86-411-84986121; E-mail: lixiang@dlut.edu.cn
This work was supported by the National Natural Science Foundation of China (20773020, 20973030, 21073022, 21173033, and U1162203), the National High Technology Reaearch and Development Program of China (863 program, 2008AA030803), the Program for New Century Excellent Talents in University (NCET-04-0275), the Fundamental Research Funds for the Central Universities (DUT13LK18), and the Specialized Research Fund for the Doctral Program of Higher Education (20100041110016).
DOI: 10.1016/S1872-2067(12)60731-1 | http://www.sciencedirect.com/science/journal/18722067 | Chin. J. Catal., Vol. 35, No. 1, January 2014

Štengl and Bakardjieva [8] found that addition of MoO_3 led to an increase in the activity of anatase for the degradation of Orange II dye in the UV and visible regions.

In the present work, MoO_3 was introduced to P25 (TiO_2, ratio of anatase to rutile of 80:20) by an incipient wetness impregnation method, and the influence of MoO_3 dispersion on the photocatalytic performance of P25 under visible light was studied using the degradation of methylene blue dye.

2. Experimental

2.1. Catalyst preparation

P25 (AR grade, Degussa, Germany) supported MoO_3 catalysts were prepared by impregnating 1 g P25 with an aqueous solution of a certain amount of $(NH_4)_6Mo_7O_{24}$ (AR grade, Sinopharm Chemical Reagent Co. Ltd.), followed by drying at 120 °C for 8 h and calcination at 500 °C in air for 5 h. The catalysts were denoted as MoO_3/P25(x), where x stands for the mass ratio of MoO_3 to P25. In the present work, the values of x were set to 0.05, 0.1, 0.15, 0.25, and 0.4.

2.2. Catalyst characterization

The structure of the catalysts was determined using a Rigaku D/Max 2400 powder X-ray diffractometer with nickel-filtered Cu-K_α radiation (λ = 0.154 nm). The specific surface areas of the samples were measured on a Micromeritics TriStar II 3020 adsorption analyzer. UV-Vis absorption data were obtained using a JASCO UV-550 spectrophotometer. IR spectra were recorded using an Equinox 55 Fourier transform infrared (FT-IR) spectrophotometer at room temperature with KBr pellets in the range 4000–400 cm^{-1}. Samples were dried in an oven (120 °C) before the measurements. A DL-2 laser Raman spectrometer (λ = 532 nm) was used to measure the Raman spectra of the catalysts.

2.3. Catalyst evaluation

A 110 W high-pressure sodium lamp was adopted as the light source for the photodegredation experiments, and the UV light portion of the lamp (λ < 400 nm) was filtered using a JB400 cut-off glass filter. An aqueous solution of methylene blue dye (15 mg/L) was used as the reactant. The catalyst (0.01 g) was dispersed in 100 mL of the methylene blue dye solution, and the reaction was conducted at 25 °C and atmospheric pressure. After stirring of the suspension for 40 min, the light was turned on and the suspension was bubbled with air. The suspension (2–3 mL) was collected every 30 min, and the supernatant was separated using centrifugation. The percentage of methylene blue dye degradation was determined based on the absorbance of the obtained supernatant solution, measured using a 721 visible spectrophotometer at a wavelength of 664 nm. A blank experiment indicated that the degradation of methylene blue dye in the presence of light irradiation but absence of catalyst was less than 10%. The amount of dye adsorbed on the catalysts was also measured in the absence of light irradiation.

3. Results and discussion

3.1. Catalyst characterization

Figure 1 shows the XRD patterns of P25, MoO_3, and MoO_3/P25(x). In the XRD pattern of P25, the diffraction peaks at 2θ = 25.6°, 38.1°, and 48.2° are assignable to the (101), (004), and (200) planes of anatase; while those at 2θ = 27.7°, 36.4°, and 45.5° correspond to the (110), (101), and (111) planes of rutile, respectively. In the case of MoO_3, the peaks at 2θ = 12.8°, 23.4°, 25.7°, and 27.3° were due to the (001), (100), (002), (011) planes of the α-MoO_3 phase, respectively. No characteristic peaks related to MoO_3 phase were clearly observed for the samples with MoO_3/P25 mass ratio of less than 0.15. Thereafter, the intensity of the peaks belonging to anatase decreased while that ascribed to the MoO_3 phase increased with MoO_3/P25 ratio. The specific surface areas of the MoO_3/P25(x) samples are listed in Table 1. The results indicate that the specific surface areas of the catalysts decreased with increasing MoO_3 loading.

Figure 2 illustrates the Raman spectra of MoO_3 and MoO_3/P25(x). In the spectrum of MoO_3, the bands at 242 and 343 cm^{-1} are due to the Mo–O–Mo deformation [9,10], and the band at 287 cm^{-1} is the result of deformation of the Mo=O bond [11]. The other three bands at 671, 820, and 996 cm^{-1} are assignable to the triply coordinated oxygen (Mo_3–O) stretching mode, which results from edge-shared oxygens in common to

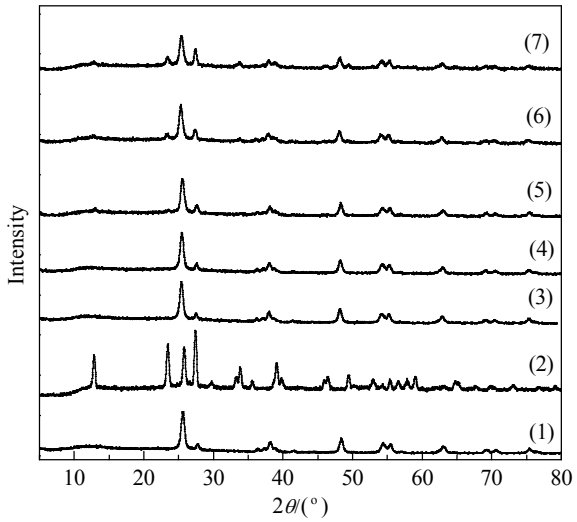

Fig. 1. XRD patterns of P25, MoO_3, and MoO_3/P25(x). (1) P25; (2) MoO_3; (3) MoO_3/P25(0.05); (4) MoO_3/P25(0.1); (5) MoO_3/P25(0.15); (6) MoO_3/P25(0.25); (7) MoO_3/P25(0.4).

Table 1
Specific surface areas of the MoO_3/P25(x) samples.

Sample	Specific surface area (m^2/g)
MoO_3/P25(0.05)	45.4
MoO_3/P25(0.1)	43.8
MoO_3/P25(0.15)	40.2
MoO_3/P25(0.25)	37.2
MoO_3/P25(0.4)	33.4

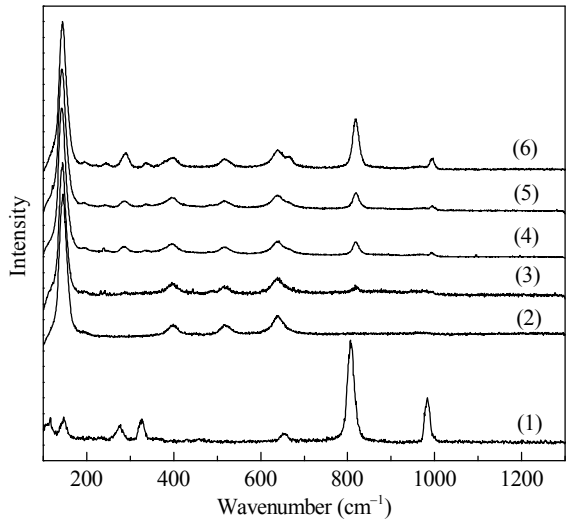

Fig. 2. Raman spectra of MoO_3 and MoO_3/P25(x). (1) MoO_3; (2) MoO_3/P25(0.05); (3) MoO_3/P25(0.1); (4) MoO_3/P25(0.15); (5) MoO_3/P25(0.25); (6) MoO_3/P25(0.4).

three MoO_6 octahedra [12], the Mo–O–Mo stretching of corner sharing MoO_6 octahedra [11], and the symmetric Mo=O stretching mode [12], respectively, in the orthorhombic α-MoO_3 phase. In the spectra of MoO_3/P25(x), the bands at 144, 397, 517, and 638 cm^{-1} are due to anatase [13], and the intensity of these bands was almost unaffected by increasing the MoO_3/P25 ratio. The characteristic bands of MoO_3 appeared in the spectra of the catalysts with MoO_3/P25 mass ratio higher than 0.1. The intensity of these bands increased with MoO_3 loading, suggesting that the Mo species aggregated to form MoO_3 clusters [14].

The FT-IR spectra of P25, MoO_3, MoO_3/P25(0.05), MoO_3/P25(0.1), and MoO_3/P25(0.15) are shown in Fig. 3. In the spectrum of MoO_3, the band at 990 cm^{-1} is characteristic of the vibration of the Mo=O terminal bond, that at 870 cm^{-1} is associated with the vibration of Mo–O–Mo bridging bonds, and the band at 620 cm^{-1} is typical of the vibration of the Mo_2O_2 entity formed by the edge shared MoO_6 polyhedra that form the orthorhombic α-MoO_3 structure [15]. In the spectra of P25 and the supported MoO_3 catalysts, the broad bands located at 521 and 668 cm^{-1} are related to the vibration of the Ti–O bond and the rotation of the Ti–O–Ti bond in P25, respectively [16]. For all the supported MoO_3 samples, the band centered at 960 cm^{-1} is attributed to the vibration of the Mo–O–Ti species, which is mainly in the tetrahedral form [17]. Compared with the similar band in the spectrum of MoO_3, the band at 996 cm^{-1} in the spectrum of MoO_3/P25(0.15) with relatively high MoO_3 loading should be assigned to the vibration of the Mo=O terminal bond [15,17,18].

Figure 4 shows the UV-Vis spectra collected from P25, MoO_3, and MoO_3/P25(x). P25 is composed of anatase and rutile. The band gap of anatase is 3.2 eV while that of rutile is 3.0 eV, neither of which has a visible light response. In contrast, MoO_3 exhibits visible light absorption because its band gap is only 2.9 eV. The absorbance of MoO_3/P25(x) for visible light was increased in comparison to that of P25, and the optimum MoO_3/P25 ratio was found to be 0.1. Above 0.1 the absorption in the visible light region decreased. It should be noted that the UV-Vis spectrum of MoO_3/P25(0.15) was similar to that of MoO_3/P25(0.25). When the MoO_3/P25 ratio was as high as 0.4, the optical absorption of the catalyst was close to that of the bulk MoO_3.

TiO_2 is an indirect band gap semiconductor. Therefore, the band gap values of the catalysts can be calculated from the UV-Vis spectra using the equation $\alpha = c(h\nu - E_g)^2/h\nu$, where c is a frequency-independent constant and α is the absorption coefficient [19]. The intercept from the extrapolation of the linear portion of the $(\alpha h\nu)^{1/2} \sim h\nu$ plot gives the band gap, E_g [14]. Figure 5 shows the plot for the calculation of the band gap using P25 as an example. The band gap calculated for P25 was 3.03 eV, which is close to the known value (around 3.1 eV), indicating that the calculation is reliable. Table 2 summarizes the calculated band gap values of the different catalysts. The band gaps of the MoO_3/P25(x) catalysts decreased with increasing MoO_3/TiO_2 mass ratio until 0.1, above which the band gap in-

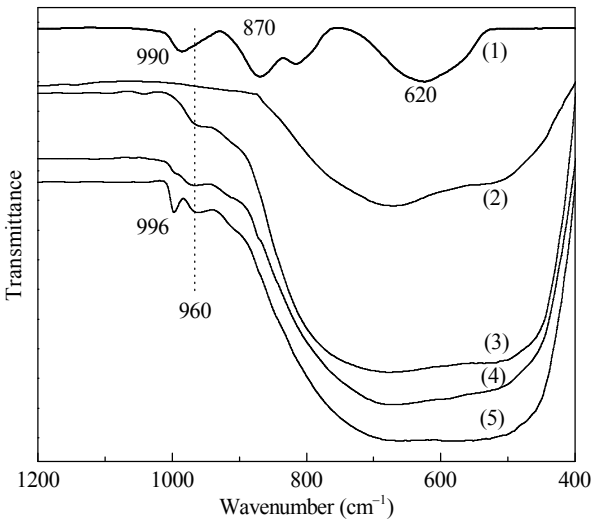

Fig. 3. FT-IR spectra of MoO_3, P25, and MoO_3/P25(x). (1) MoO_3; (2) P25; (3) MoO_3/P25(0.05); (4) MoO_3/P25(0.1); (5) MoO_3/P25(0.15).

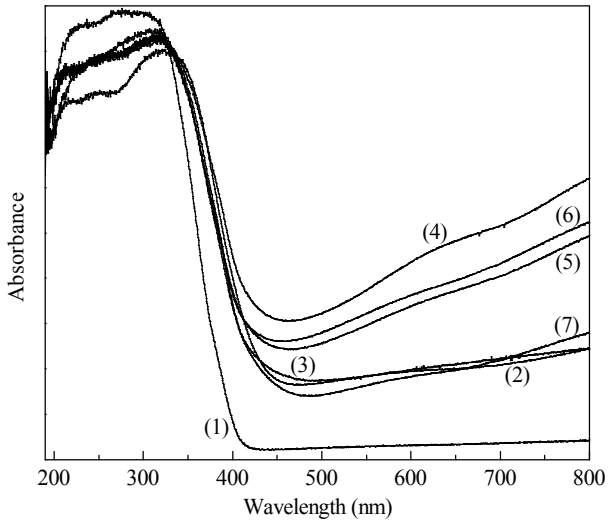

Fig. 4. UV-Vis spectra of P25, MoO_3, and MoO_3/P25(x). (1) P25; (2) MoO_3; (3) MoO_3/P25(0.05); (4) MoO_3/P25(0.1); (5) MoO_3/P25(0.15); (6) MoO_3/P25(0.25); (7) MoO_3/P25(0.4).

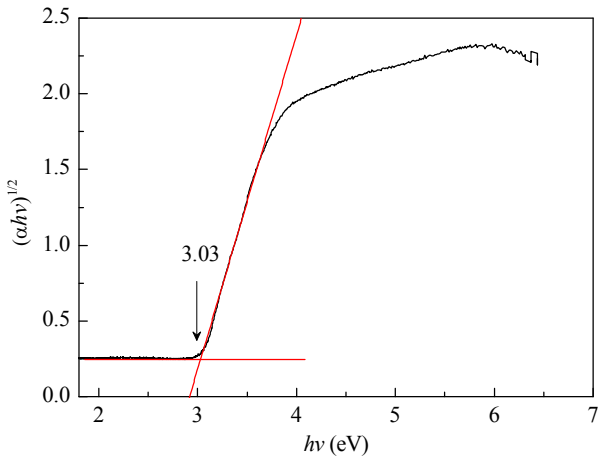

Fig. 5. Plot for the calculation of the band gap of P25.

Table 2
Band gaps of the MoO_3/P25(x) samples.

Sample	Band gap (eV)
MoO_3/P25(0.05)	2.55
MoO_3/P25(0.1)	2.16
MoO_3/P25(0.15)	2.21
MoO_3/P25(0.25)	2.26
MoO_3/P25(0.4)	2.45

creased with MoO_3/TiO_2 mass ratio.

The characterization results indicated that the monolayer dispersion threshold of MoO_3 on P25 was around 0.1 g/g. This value is in accordance with that reported in the literature. There are strong interactions between MoO_3 and TiO_2, and the maximum dispersion capacity of MoO_3 on TiO_2 should agree with the value according to a close-packed monolayer model [20]. The Mo surface packing density is 6.8×10^{18} /m^2 [14], which is equal to MoO_3 0.0017 g/m^2. The specific surface area of P25 adopted in the present work was 47 m^2/g. Therefore, the theoretical MoO_3/TiO_2 mass ratio corresponding to the monolayer dispersion threshold should be 0.08. Both the Raman (Fig. 2) and FT-IR (Fig. 3) measurements confirmed that when the MoO_3/TiO_2 mass ratio was higher than 0.1, the Mo species on the surface of P25 grew and aggregated to form a crystalline MoO_3 phase. Based on the UV-Vis results, the visible light absorption of P25 was significantly enhanced by the monolayer dispersed Mo species. The catalysts not only showed visible light absorbance, but an absorbance that was even higher than that of MoO_3. The formation of the Mo–O–Ti bond between the monolayer dispersed Mo species and TiO_2 (Fig. 3) would be one of the reasons accounting for the enhancement. The electronic transition between TiO_2 and MoO_3 is symmetry forbidden [21,22]. Once the Mo–O–Ti bond formed at the interface of MoO_3 and TiO_2, the symmetry may have been reduced, and the electron transfer from the valence band (VB) of TiO_2 to the conduction band (CB) of MoO_3 would have become possible due to the charge transfer properties of Mo–O–Ti [22]. Because the band gap between the VB of TiO_2 and the CB of MoO_3 is in the energy range of visible light [14,22], the visible light absorption of the catalysts was improved. Further increase in the MoO_3 loading led to the formation of crystalline MoO_3, which may have reduced the interaction between the Mo species and TiO_2, and thus the visible light absorption of the catalysts.

3.2. Catalytic degradation of methylene blue dye under visible light

The degradation of methylene blue dye under visible light was used as the probe reaction to evaluate the visible light photocatalytic activity of P25, MoO_3, and MoO_3/P25(x). The results are presented in Fig. 6. The conversion of methylene blue dye over P25 and MoO_3 was less than 8%, indicating that the two catalysts possessed low photocatalytic activity under visible light. The addition of MoO_3 led to an increase in the activity of P25, and the optimum MoO_3/TiO_2 mass ratio was found to be 0.25. After 150 min reaction under visible light over MoO_3/P25(0.25), the conversion of methylene blue dye reached 38%. There was no close relation between the specific surface areas (Table 1) of the catalysts and their photocatalytic activity, suggesting that the specific surface area cannot be the key factor determining the performance of the catalysts. Combined with the characterization results, the band gap or the visible light absorption of the catalysts seems to be not the only factor affecting their activity. MoO_3 is an acidic semiconductor [23], while methylene blue dye is a basic dye. Although the visible light absorption of the catalysts with high MoO_3 loading was low, the adsorption of the substrate on these catalysts was strong. Figure 7 shows the variation of the relative methylene blue concentration during its adsorption over MoO_3 and MoO_3/P25(x). Either the adsorption rate (the slope of the curve) or the adsorption capacity of the catalysts increased with MoO_3 content, indicating that the adsorption of methylene blue dye on MoO_3/P25(x) increased with MoO_3 loading. Hence, MoO_3/P25(0.25), which not only possessed a suitable band gap but also a certain amount of crystalline MoO_3, showed the best catalytic performance.

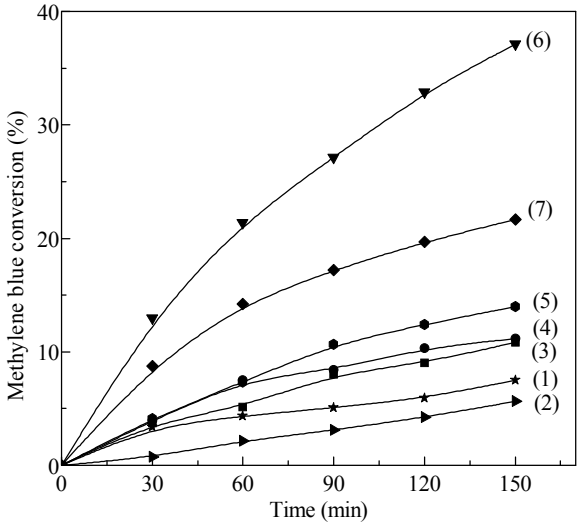

Fig. 6. Photocatalytic activity of P25, MoO_3, and MoO_3/P25(x) under visible light. (1) P25; (2) MoO_3; (3) MoO_3/P25(0.05); (4) MoO_3/P25(0.1); (5) MoO_3/P25(0.15); (6) MoO_3/P25(0.25); (7) MoO_3/P25(0.4).

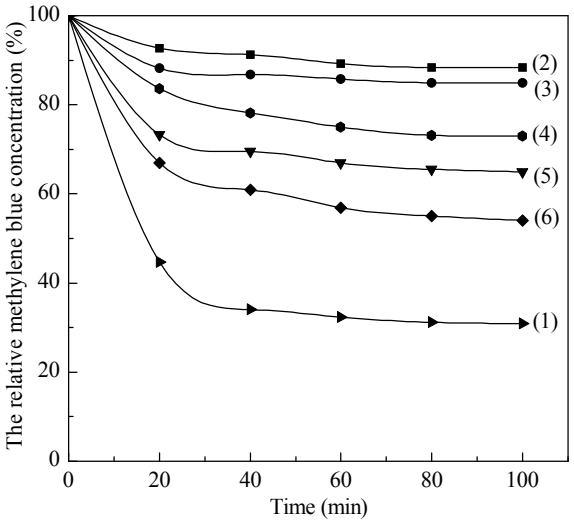

Fig. 7. Variation of the relative methylene blue concentration during its adsorption over MoO_3 and MoO_3/P25(x). (1) MoO_3; (2) MoO_3/P25(0.05); (3) MoO_3/P25(0.1); (4) MoO_3/P25(0.15); (5) MoO_3/P25(0.25); (6) MoO_3/P25(0.4).

4. Conclusions

The monolayer dispersion threshold of MoO_3 on P25 was around 0.1 g/g. The interaction between the monolayer-dispersed molybdenum oxide species and P25 was strong, leading to a decrease in the band gap of P25, and thus an increase in visible light absorption. Crystalline MoO_3 was formed on the catalysts having a MoO_3/P25 mass ratio above 0.1, which may have reduced the interaction between the molybdenum oxide species and TiO_2. In these cases, the visible light absorption of the catalysts decreased with increasing MoO_3 content. The optimum MoO_3/P25 mass ratio of the MoO_3/P25(x) catalysts for the degradation of methylene blue dye under visible light was found to be 0.25. This suggests that not only the visible light absorption but also the adsorption of the substrate influenced the activity of the catalysts. MoO_3/P25(0.25), which not only possessed a suitable band gap but also a certain amount of crystalline MoO_3, showed the best catalytic performance.

References

[1] Takeda K, Fujiwara K. *Water Res*, 1996, 30: 323
[2] Wang C M, Heller A, Gerischer H. *J Am Chem Soc*, 1992, 114: 5230
[3] Litter M I, Navio J A. *J Photochem Photobiol A*, 1996, 98: 171
[4] Kamat P V. *Chem Rev*, 1993, 93: 267
[5] Zhang J L, Chen F, He B. Photocatalysis. Shanghai: East China Univ Sci Technol Press (张金龙, 陈锋, 何斌. 光催化. 上海: 华东理工大学出版社), 2004. 84
[6] Liu Y, Wang S P, Ma X B. *Ind Eng Chem Res*, 2007, 46: 1045
[7] Kubacka A, Colon G, Fernandez-Garcia M. *Catal Today*, 2009, 143: 286
[8] Štengl V, Bakardjieva S. *J Phys Chem C*, 2010, 114: 19308
[9] Panagiotou G D, Petsi T, Bourikas K, Kalampounias A G, Boghosian S, Kordulis C, Lycourghiotis A. *J Phys Chem C*, 2010, 114: 11868
[10] Bergwerff J A, Visser T, Leliveld B R G, Rossenaar B D, de Jong K P, Weckhuysen B M. *J Am Chem Soc*, 2004, 126: 14548
[11] Santos E B, de Silva J M, Mazali I O. *Vib Spectrosc*, 2010, 54: 89
[12] Lee S H, Seong M J, Tracy C E, Mascarenhas A, Pitts J R, Deb S K. *Solid State Ionics*, 2002, 147: 129
[13] Zhang J, Li M J, Feng Z C, Chen J, Li C. *J Phys Chem B*, 2006, 110: 927
[14] Elder S H, Cot F M, Su Y, Heald S M, Tyryshkin A M, Bowman M K, Gao Y, Joly A G, Balmer M L, Kolwaite A C, Magrini K A, Blake D M. *J Am Chem Soc*, 2000, 122: 5138
[15] Stoyanova A, Iordanova R, Mancheva M, Dimitriev Y. *J Optoelectron Adv Mater*, 2009, 11: 1127
[16] Lopez T, Ortiz E, Gomez R, Picquart M. *J Sol-Gel Sci Technol*, 2006, 37: 189
[17] Li C, Xin Q, Wang K L, Guo X X. *Appl Spectrosc*, 1991, 45: 874
[18] Han W P, Yin X L, Li Y Z. *Chin J Catal* (韩维屏, 尹喜林, 李永战. 催化学报), 1992, 13: 19
[19] Ma H L, Xue C S. Nano Semiconductors. Beijing: National Defence Industry Press (马洪磊, 薛成山. 纳米半导体. 北京: 国防工业出版社), 2009. 306
[20] Liu Y J, Xie Y C, Xie G, Tang Y Q. *Chin J Catal* (刘英俊, 谢有畅, 解刚, 唐有祺. 催化学报), 1985, 6: 101
[21] Sang L X, Zhong S H, Xiao X F, Wang X T, Tan J H, Zhou Z Q. *Chem J Chin Univ* (桑丽霞, 钟顺和, 肖秀芬, 王希涛, 谭建华, 周智泉. 高等学校化学学报), 2004, 25: 1115
[22] Wang J, Zhang G J, Yang W S, Yao J N. *Acta Chim Sin* (王静, 张光晋, 杨文胜, 姚建年. 化学学报), 2005, 63: 1951
[23] Song K Y, Park M K, Kwon Y T, Lee H W, Chung W J, Lee W I. *Chem Mater*, 2001, 13: 2349

Graphical Abstract

Chin. J. Catal., 2014, 35: 140–147 doi: 10.1016/S1872-2067(12)60731-1

Photocatalytic degradation of methylene blue by MoO_3 modified TiO_2 under visible light

Huabo Yang, Xiang Li *, Anjie Wang, Yao Wang, Yongying Chen
Dalian University of Technology

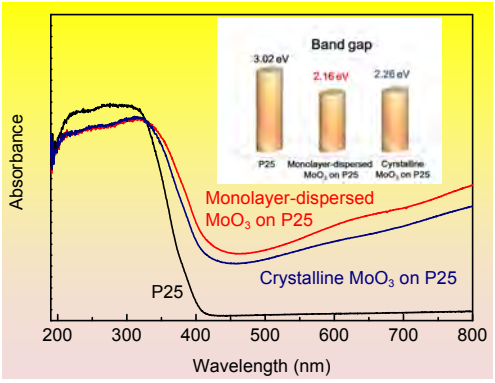

Strong interactions between the monolayer-dispersed tetrahedral-coordinated molybdenum oxide species and P25 lead to a decrease in the band gap of P25, and thus an increase in its visible light absorption.

MoO_3改性的TiO_2在可见光下催化降解亚甲基蓝

杨华博[a], 李　翔[a,b,*], 王安杰[a,b], 王　瑶[b], 陈永英[b]
[a]大连理工大学化工学院精细化工国家重点实验室, 辽宁大连116024
[b]辽宁省省级高校石油化工技术与装备重点实验室, 辽宁大连116024

摘要: 采用浸渍法制备了MoO_3/P25催化剂(MoO_3/P25(x), x为MoO_3与P25质量比), 用X射线衍射、紫外-可见漫反射光谱、傅里叶变换红外光谱及拉曼光谱等手段对样品进行了表征, 并用催化降解亚甲基蓝考察了催化剂在可见光区的催化活性. 结果表明, MoO_3在P25表面最大单层负载量对应的MoO_3与P25质量比在0.1左右. 单层分散的氧化钼物种与P25之间有较强的相互作用, 降低了P25禁带宽度, 提高了催化剂对可见光的吸收. 当MoO_3与P25质量比大于0.1时, 会生成晶相MoO_3, 催化剂对可见光的吸收反而随MoO_3担载量增加而降低. 催化剂禁带宽度不是决定其可见光下催化降解亚甲基蓝活性的唯一因素. 具有适宜禁带宽度和一定晶相MoO_3含量的MoO_3/P25(0.25)表现出最佳活性.

关键词: 二氧化钛; 氧化钼; 等体积浸渍; 亚甲基蓝; 可见光

收稿日期: 2013-07-14. 接受日期: 2013-10-09. 出版日期: 2014-01-20.
*通讯联系人. 电话: (0411)84986124; 传真: (0411)84986121; 电子信箱: lixiang@dlut.edu.cn
基金来源: 国家自然科学基金(20773020, 20973030, 21073022, 21173033和U116220320503003); 国家高技术研究发展计划(863计划, 2008AA030803); 教育部新世纪优秀人才支持计划(NCET-04-0275); 中央高校基本科研业务费专项资金(DUT13LK18); 高等学校博士学科点专项科研基金(20100041110016).
本文的英文电子版由Elsevier出版社在ScienceDirect上出版(http://www.sciencedirect.com/science/journal/18722067).

1. 前言

TiO_2是最常用的光催化剂. 它成本低, 化学性质稳定, 并且具有很高的氧化能力, 能够将绝大多数有机污染物降解并最终完全矿化为CO_2, H_2O及其它无机小分子物质, 从而消除污染. 但是, 它的禁带宽度(3.0–3.2 eV)较大, 需要能量较高的紫外线照射才能表现出光催化活性, 而且量子产率较低. 为提高TiO_2对可见光的响应, 有效利用太阳能, 人们主要从降低TiO_2禁带宽度能和提高量子效率两方面对其进行改性. 常用的方法包括贵金属沉积[1,2], 离子掺杂[3], 半导体复合[4]以及有机物光敏化[5]等. MoO_3的带隙能为2.9 eV, 与TiO_2接近. 它与TiO_2之间有较强的相互作用[6]. 很多文献报道掺杂MoO_3可以在一定程度上提高TiO_2在紫外和可见光区的光电催化活性. 如Kubacka等[7]的研究表明TiO_2掺杂V, Mo, Nb和W后形成的混合氧化物具有均一的锐钛矿结构, 带宽显著降低, 具有较高的可见光光催化活性. Štengl等[8]报道可以通过掺杂MoO_3显著提高锐钛矿TiO_2紫外和可见光区降解橙II染料的活性.

本文采用等体积浸渍法将MoO_3负载在P25(TiO_2, 锐钛矿相和金红石相比例为80:20)上, 以光催化降解亚甲基蓝作为探针反应, 研究了Mo物种分散状态对P25可见光催化活性的影响.

2. 实验部分

2.1. 催化剂的制备

采用等体积浸渍法将一定量的钼酸铵(分析纯, 国药集团化学试剂有限公司)均匀负载在1 g的P25 (分析纯, Degussa, 德国)上, 120 ºC干燥8 h, 然后在500 ºC下焙烧5 h制得催化剂, 记为MoO_3/P25(x), 其中x为MoO_3和P25的质量比(x = 0.05, 0.1, 0.15, 0.25和0.4).

2.2. 催化剂的表征

采用日本理学D/MAX-2400型X射线衍射仪(Cu K_α靶, λ = 0.154 nm)测定催化剂的结构. 样品比表面积用Micromeritics公司TriStar II 3020型全自动比表面积和孔隙度分析仪测定. 用日本JASCO公司UV-550型紫外-可见漫反射光谱仪(UV-Vis)测定催化剂对可见和紫外光的吸收. 红外光谱采用德国布鲁克公司EQUINOX 55型傅立叶变换红外光谱(FT-IR)仪测定. 样品在干燥箱中(120 °C)干燥后与KBr混合压片, 室温下测试, 光谱范围: 4000–400 cm^{-1}. 采用DL-2型激光拉曼(Raman)光谱仪测定催化剂的Raman谱图, 激发光λ = 532 nm.

2.3. 催化剂的评价

光源为110 W的高压钠灯, 用截止型滤光片JB400滤掉λ < 400 nm的光. 采用浓度为15 mg/L的亚甲基蓝水溶液作为反应物. 取0.01 g催化剂加入到100 mL亚甲基蓝水溶液中, 控制反应温度25 ºC. 在常压下搅拌40 min后开始进行光照, 并通过空气泵向反应体系内鼓入空气. 每隔30 min取上层清液(2–3 mL), 离心分离后用721型可

见光分光光度计在664 nm波长处测定溶液的吸光度, 并计算出亚甲基蓝的降解率. 空白实验表明, 在光照无催化剂时, 相同条件下亚甲基蓝的降解率小于10%. 此外, 还在无光照条件下测定了亚甲基蓝在催化剂上的吸附.

3. 结果与讨论

3.1. 催化剂表征结果

图1是P25, MoO_3及MoO_3/P25(x)样品的XRD谱. 在P25谱中, $2\theta = 25.6^o$, 38.1^o和48.2^o的衍射峰分别对应于锐钛矿相(101), (004)和(200)晶面; $2\theta = 27.7^o$, 36.4^o和45.5^o分别对应于金红石相(110), (101)和(111)晶面衍射峰. 而在MoO_3谱中, $2\theta = 12.8^o$, 23.4^o, 25.7^o和27.3^o的峰分别对应α-MoO_3的(001), (100), (002)和(011)晶面. 在MoO_3/P25质量比低于0.15的样品的XRD谱中没有明显的MoO_3特征峰. 之后, 随着MoO_3/P25质量比增加, 锐钛矿特征峰强度减弱, MoO_3的特征衍射峰逐渐增强. MoO_3/P25(x)样品的比表面积列于表1, 催化剂比表面积随着MoO_3担载量增加而降低.

图2示出了MoO_3及MoO_3/P25(x)的Raman谱. 在MoO_3的Raman谱图中, 242和343 cm^{-1}吸收峰为Mo–O–Mo变形振动[9,10], 而287 cm^{-1}处的峰则归属为Mo=O的变形振动[11]; 671, 820和996 cm^{-1}处吸收峰分别归属为α-MoO_3的共边连接钼氧八面体中Mo–O伸缩振动[12], 共顶点连接钼氧八面体中的Mo–O伸缩振动[11]以及末端Mo=O对称伸缩振动[12]. 在MoO_3/P25(x)的谱中, 144, 397, 517和638 cm^{-1}处的吸收峰可归属为锐钛矿的特征峰[13]; 随着MoO_3/P25质量比的增大, 归属为锐钛矿的特征峰强度几乎不变. 当MoO_3与P25质量比大于0.1时开始出现MoO_3的特征峰, 并且随担载量的增加而增加, 说明Mo物种逐步形成聚集态的MoO_3簇[14].

图3为各催化剂在波数400–1200 cm^{-1}范围的FT-IR谱. 在MoO_3样品上, 990 cm^{-1}处的吸收峰为MoO_3相末端Mo =O伸缩振动, 870 cm^{-1}处的吸收峰对应Mo–O–Mo桥键的振动, 而620 cm^{-1}处的吸收峰则为共边的MoO_6多面体(构成α-MoO_3的结构单元)形成的Mo_2O_2物种的振动峰[15]. 在P25及其担载MoO_3的样品中, 521和668 cm^{-1}处的宽大吸收峰分别归属为P25中Ti–O键的振动和Ti–O–Ti的转动[16]. 在所有负载MoO_3的样品中, 960 cm^{-1}处的吸收峰为四面体配位的Mo–O–Ti键的振动[17]. 根据MoO_3的红外光谱, 在MoO_3含量较高的MoO_3/P25(0.15)样品中, 996 cm^{-1}处吸收峰应归属MoO_3晶相末端Mo=O的伸缩振动[15,17,18].

图4为P25, MoO_3以及MoO_3/P25(x)的UV-Vis谱. P25由锐钛矿和金红石两相组成, 锐钛矿的禁带宽度为3.2 eV, 金红石为3.0 eV, 二者在可见光下都没有响应. MoO_3的禁带宽度为2.9 eV, 在可见光下有一定吸收. 负载MoO_3后MoO_3/P25(x)对可见光的吸收有不同程度的提高, 其中MoO_3/P25(0.1)对可见光的吸收最强. 随MoO_3含量增加, 催化剂对可见光的吸收降低. 其中, MoO_3/P25(0.15)与MoO_3/P25(0.25)对光的吸收性质相近, 但当MoO_3/TiO_2质量比达到0.4时, 催化剂对紫外和可见光的吸收与体相MoO_3基本相同.

TiO_2为间接带隙半导体. 根据半导体表观光学带隙与UV-Vis吸收系数的关系$\alpha = c(h\nu - E_g)^2/h\nu$ (c为吸收常数, α为吸收系数[19])绘制$(\alpha h\nu)^{1/2}$~$h\nu$曲线, 取该曲线中直线部分截距可以得到催化剂的禁带宽度E_g[14]. 图5以P25为例示出了禁带宽度计算示意图. 计算得到的P25禁带宽度为3.03 eV, 与已知的P25禁带宽度(约3.1 eV)相近, 说明计算方法可靠. 表2列出了不同MoO_3/P25(x)催化剂的禁带宽度. 当MoO_3/TiO_2质量比小于0.1时, 禁带宽度随着质量比的增大而减小; 当MoO_3/TiO_2质量比大于0.1时, 禁带宽度随着质量比增大而增大.

由以上表征结果可以看出, MoO_3在P25上达到最大单层负载时对应的MoO_3/TiO_2质量比应在0.1左右. 这与文献报道值相近. TiO_2与MoO_3的相互作用较强, MoO_3在TiO_2上的单层分散量等于理论密置单层容量[20]. MoO_3在TiO_2表面单层覆盖时的表面密度为6.8×10^{18}/m^2 [14], 换算后MoO_3为0.0017 g/m^2. 本文选用的P25比表面积为47 m^2/g, 则MoO_3在P25表面达到最大单层负载时MoO_3/TiO_2质量比的理论值为0.08. 拉曼光谱(图2)和红外光谱(图3)表明, 当MoO_3/TiO_2质量比大于0.1时, Mo物种在P25表面团聚长大为晶相的MoO_3. 结合UV-Vis光谱结果可以看出, 单层分散的Mo物种显著提高了P25对可见光的吸收. 这时催化剂不仅对可见光有了吸收, 而且对可见光吸收强度大于MoO_3. 单层分散的氧化钼物种与TiO_2之间形成Mo–O–Ti键(图3)可能是提高催化剂对可见光吸收的原因之一. TiO_2和MoO_3之间的跃迁是对称禁阻的[21,22]. 但如果在TiO_2与MoO_3复合界面上生成Mo–O–Ti键, 由于Mo–O–Ti键具有电荷转移特性, 则会打破这种跃迁上的禁阻, 使从TiO_2价带到MoO_3导带的电子跃迁变得可能[22]. 而从TiO_2价带到MoO_3导带的带隙恰好落在可见光吸收区间内[14,22], 因此提高了催化剂对可见光的吸收. 随着MoO_3含量的增加, 在催化剂表面团聚生成MoO_3晶相后, 降低了Mo物

种与TiO_2之间相互作用, 催化剂对可见光的吸收也随之降低.

3.2. 可见光下亚甲基蓝催化降解

以可见光下催化降解亚甲基蓝作为探针反应评价了P25, MoO_3及MoO_3/P25(*x*)催化剂的可见光催化活性, 结果示于图6. 由图可见, 以P25和MoO_3作催化剂时, 亚甲基蓝转化率小于8%, 说明二者具有较低的可见光催化活性. 负载MoO_3提高了催化剂活性, 最佳MoO_3/P25质量比为0.25. 可见光下反应150 min后, 亚甲基蓝在MoO_3/P25(0.25)上的转化率达到了38%. 催化剂的光催化活性和其比表面积(表1)之间没有必然联系, 说明催化剂比表面积不是决定其活性的关键. 结合表征结果可以看出, 催化剂的带宽或对可见光的吸收也不是决定其活性的唯一因素. MoO_3是酸性半导体[23], 而亚甲基蓝是碱性染料. MoO_3担载量较高的催化剂虽然对可见光的吸收有所降低, 但对底物的吸附较强. 图7为亚甲基蓝在MoO_3及MoO_3/P25(*x*)上吸附时浓度随时间的变化. 可以看出, 亚甲基蓝吸附量和吸附速率(曲线斜率)随MoO_3含量增加而增加, 说明MoO_3/P25(*x*)对亚甲基蓝的吸附随MoO_3含量增加而增强. 因此, 具有适宜带宽和MoO_3担载量的MoO_3/P25(0.25)表现出最佳的活性.

4. 结论

MoO_3在P25表面最大单层负载量对应的MoO_3/P25质量比在0.1左右. 单层分散的氧化钼物种与P25之间有较强的相互作用, 降低了P25禁带宽度, 提高了催化剂对可见光的吸收. 而当MoO_3/P25质量比大于0.1时, 会生成晶相MoO_3, 削弱了氧化钼物种与TiO_2之间的相互作用, 催化剂对可见光的吸收反而随MoO_3担载量增加而降低. 对于可见光下降解亚甲基蓝反应, 最佳的MoO_3/P25质量比为0.25, 说明催化剂活性不仅取决于其对可见光的吸收, 可能还与反应底物在催化剂表面的吸附有关. 具有适宜禁带宽度和一定晶相MoO_3含量的MoO_3/P25(0.25)表现出最佳反应性能.